Separated boundary layer transition under pressure gradient in the presence of free-stream turbulence

Hua J. Li [a] (李华君) and Zhiyin Yang [b] (杨志垠)
[a] Department of Engineering and Design, School of Engineering and Informatics,
University of Sussex, Brighton, UK
[b] School of Mechanical Engineering and the Built Environment,
College of Engineering and Technology, University of Derby, Derby, UK

[b] Author to whom correspondence should be addressed: Z.Yang@Derby.ac.uk. Tel: +44 (0)1332 593588

ABSTRACT

Large-eddy simulation (LES) has been carried out to investigate the transition process of a separated boundary layer on a flat plate. A streamwise pressure distribution is imposed to mimic the suction surface of a low-pressure turbine (LPT) blade and the free-stream turbulence intensity at the plate leading edge is 2.9%. A dynamic sub-grid scale model is employed in the study and the current LES results compare well with available experimental data and previous LES results. The transition process has been thoroughly analysed and streamwise streaky structures, known as the Klebanoff Streaks have been observed much further upstream of the separation. However, transition occurs in the separated shear layer and is caused by two mechanisms: streamwise streaks and the inviscid K-H instability. Analysis suggests that streamwise streaks paly a dominant role in the transition process as those streaks severely disrupt and break up the K-H rolls once they are formed, leading to significant three-dimensional (3D) motions very rapidly. It is also demonstrated in the present study that the usual secondary instability stage under low free-stream turbulence intensity where coherent two-dimensional (2D) spanwise rolls get distorted gradually and eventually broken up into 3D structures has been bypassed.

Keywords: Separated boundary layer transition; instability; Large-eddy simulation; pressure gradient; free-stream turbulence.

1. INTRODUCTION

Laminar boundary layer separation and transition can be found in many engineering flows and its behaviour strongly influences the aerodynamics and heat transfer characteristics of those flow systems. A laminar boundary layer on a smooth surface may separate due to an adverse pressure gradient or as a result of sudden surface curvature change, and under low level of flow disturbances the separated shear layer becomes unstable via an inviscid instability mechanism: Kelvin-Helmholtz (K-H) instability [1 - 13]. Nevertheless, it is demonstrated that despite the dominant role played by the K-H instability in the transition process the viscous Tollmien-Schlichting (T-S) instability may also be active [14 - 18], and there is likely an interaction between those two instabilities.

For attached boundary layers in the presence of significant flow disturbances such as free-stream turbulence it is well known that transition occurs very rapidly and the 2D viscous instability stage of the transition process (T-S instability) is bypassed, and hence termed as "bypass transition" [19 - 26]. For separated boundary layers Walker [27] argued in the early 1990s that bypass transition, similar to that in an attached boundary layer, could occur too under high level of flow disturbances. However, transition process in a separated boundary layer is much more complex and it is very vague what "bypass transition" precisely means. Does it mean that the dominant K-H instability is bypassed? Or the T-S instability is bypassed since the T-S instability could be active too? Or both the K-H and T-S instabilities are bypassed? Yang [28, 29] clarified this in a recent review paper by classifying separated boundary layer transition into two categories depending on how separation happens: i) separation induced by an adverse pressure gradient; ii) separation induced geometrically.

In the first category an attached boundary layer develops over a certain distance before it separates and "bypass transition" was used by some

researchers to describe the transition process. However "bypass" here does not mean that the K-H instability stage is bypassed. It was shown by McAuliffe and Yaras [9] for a separated boundary layer transition in the presence of free-stream turbulence (1.5% at the mean separation point) that the K-H instability is still active. Nevertheless they [9] did point out that the receptivity mechanism leading to separated shear layer roll-up is bypassed as a result of the boundary layer streaks formed upstream interacting with the separated shear layers. Bazel and Fasel [30] demonstrated that at elevated free-stream turbulence levels up to 2.5% streaky structures were observed in the laminar boundary layer upstream of the separation bubble and transition was due to both the primary inviscid shear-layer instability (K-H instability) and the streamwise streaks caused by the free-stream turbulence. Istvan and Yarusevych [31] performed experiments to investigate the effects of free-stream turbulence on transition in a laminar separation bubble formed over the suction side of a NACA 0018 airfoil at a Reynolds number of 80,000. Four cases under different free-stream turbulence intensity levels (0.06%, 0.32%, 0.51%, 1.99%) were considered and their results show that the shear layer rolls up into vortices which are shedded further downstream. Even for the highest free-stream turbulence intensity case (1.99%) the shear layer roll-up/vortex shedding is still clearly observable, which strongly indicates that the inviscid shear layer instability (K-H instability) is still at work. However, their Proper Orthogonal Decomposition (POD) analysis demonstrate that for the highest free-stream turbulence intensity case, the streamwise streaks propagating from the boundary layer upstream of the bubble play an important role in the transition process as a higher percentage of the turbulent kinetic energy is generated by the streaks rather than the spanwise rollers. This confirms the findings of Bazel and Fasel [30] that transition occurs due to both the primary inviscid shear-layer instability (KH instability) and the streamwise streaks caused by the free-stream turbulence.

Simoni *et al.* [32] carried out experiments to investigate the effects of free-stream turbulence up to 2.87% on the structure and dynamic properties of a laminar separation bubble at three different Reynolds numbers (40,000; 75,000; 90,000). It was found that the K-H instability was still present under the free-stream turbulence intensity of 2.87% at Reynolds numbers of 40, 000 and 75, 000. However, as the Reynolds number was increased to 90,000 they did not detect the presence of the K-H instability since the separation bubble was already eliminated. It was also shown by Zaki *et al*. [33] that when the free-stream turbulence was about 5.5% at a compressor blade leading edge, the separation on the suction surface was eliminated completely and the transition was indeed dominated by the bypass mechanism of an attached boundary layer. This is consistent with other studies [34, 35], confirming that separation is indeed eliminated in the presence of sufficiently high free-stream turbulence and "bypass transition" occurs but "bypass" here means that the T-S instability is bypassed, not the K-H instability which is not relevant anymore in such a case because the separated shear layer does not exist at all due to the elimination of separation bubbles.

When separation is induced geometrically such as due to a sudden surface curvature change, the separation point is usually fixed with a very short distance for the development of an attached boundary layer before separation, and separation always occurs no matter what the free-stream turbulence intensity level is. In this case at low free-stream turbulence it has been demonstrated that transition is initiated by only one instability mechanism – the K-H instability [2 - 6, 8]. Unfortunately the literature on the instability mechanism in the presence of elevated free-stream turbulence is very scarce. Only Langari and Yang [36] clearly demonstrated that indeed the K-H instability is bypassed under 5.6% free-stream turbulence level for a separated boundary layer transition on a flat plate with a semi-circular leading edge.

The main goal of the current study is to further shed light on the highly complex flow physics of separated boundary layer transition on a flat plate (separation is caused by an adverse pressure gradient) subject to a free-stream turbulence level of 2.9% at the plate leading edge. In particular to complement and to advance our understanding of the above discussed issues: is the K-H instability still the dominant instability mechanism or not? is it bypassed? It is likely that the T-S instability is bypassed under such a free-stream turbulence level and if so what role will the streaky structures play in the transition process? How do the streaky structures interact with the H-K instability?

The paper is structured as follows: in section 2 flow configuration is introduced and the numerical method used in the present study is presented in section 3. Section 4 shows the mean results and comparison with experimental data, and further analysis of instantaneous flow fields to elucidate the transition process. Conclusion is drawn in section 5.

2. FLOW CONFIGURATION

The present study examines a separated boundary layer transition under an imposed streamwise pressure distribution on a flat plate (plate thickness d = 12.8 mm) with an elliptic leading edge. The pressure distribution is generated by a specific contour wall as shown in Figure 1 to mimic the pressure distribution of the T106 high-lift turbine blade. The geometry and flow conditions in the present study are selected to match as closely as possible to those used in the experiments by Coull and Hodson [37] so that the current LES results can be validated against the experimental data, which were also used for validation in a previous LES study by Nagabhushana *et al.* [38].

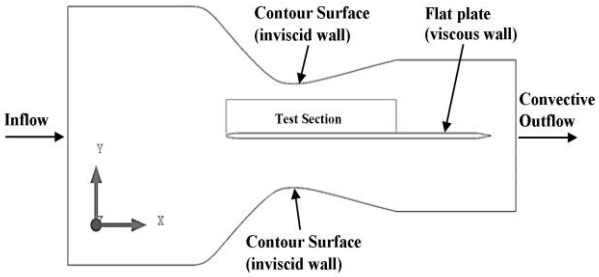

FIG. 1. Computational domain and boundaries.

The computational domain has a streamwise length of 1315 mm and spanwise size of 100mm which should be more than sufficient to capture the largest flow structures in the spanwise direction according to previous studies [3, 36]. In the vertical direction the inlet height is 644 mm and the outlet height is 377 mm. The co-ordinate system origin is at the leading edge point (stagnation point) and the inlet boundary is located upstream at -465 mm. It is worth pointing out that all important flow features occur in a region named as "Test Section" as shown in Figure 1. The length of this section is S_0 = 500mm and the value of S_0 is used to normalise all lengths in the present study in the same way as in the experimental study. A uniform velocity, U_x = 1.34 m/s, is applied at the inlet. This yields a time-mean streamwise velocity, U_{out} = 2.5 m/s, at the test section nominal exit (x/S_o = 1) matching the Reynolds number of 84,000 in the experiments defined as:

$$Re_{S_o} = \frac{U_{out} S_o}{v} \quad (1)$$

3. NUMERICAL METHOD AND COMPUTATIONAL DETAILS

An in-house finite volume LES code, with multi-block curvilinear structured co-located grid is used. Rhie-Chow pressure smoothing is employed to suppress pressure-velocity decoupling. The 2nd order central differencing scheme is used for spatial discretization and a single stage backwards Euler scheme is used for temporal discretization. The SIMPLE algorithm is used to relate the discrete face velocities from the continuity equation to the discrete pressure field in the momentum equation. A dynamic sub-grid-scale (SGS) model based on Germano *et al.* [39] and Lilly [40] is employed. More details of this CFD code can be found elsewhere [41, 42].

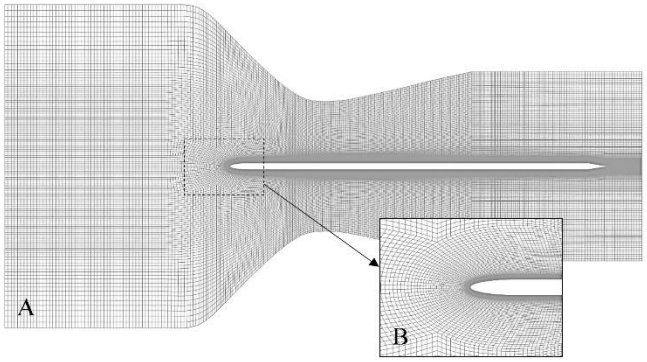

FIG. 2. A: Overview of the mesh, B: detailed view of the mesh around the flat plate leading edge.

To achieve a good mesh resolution in the important flow region the computational domain is divided into outer and inner region with a total of about 5 million cells as shown in Figure 2A. The outer region covers most of the freestream flow region and the number of mesh points in *x*, *y*, *z* directions are (428, 130, 50), slightly more than half of the total mesh points. The inner region with refined mesh covers mainly the boundary layer and separated shear layer region as shown in Figure 2B.

Based on the friction velocity much further downstream at x/S_o = 1.5, $\Delta y^+ \approx 0.9$ for the nearest cell to the wall, the streamwise mesh resolution inside the test section, Δx^+, changes from 6 to about 15 and the spanwise mesh resolution $\Delta z^+ \approx 20$. This could be regarded as "well resolved LES" and the impact of SGS model is minimal. The time step size of 1.0^{-4} second is used to ensure that the maximum CFL number is below 0.3.

It is well known in LES that a proper specification of realistic inflow turbulence is essential. There are many methods developed for generating inflow turbulence [43, 44] but none is very satisfactory. In order to generate the desirable free-stream turbulence intensity level, a so called numerical tripping method [36, 41] is used in the present study. In this approach, the turbulence generation happens inside the domain instead of at the inlet plane. A tripping plane parallel to the inlet plane is located a few cells distance downstream of inlet boundary. After initial damping of uncorrelated high frequency contents, realistic turbulence is sustained as can be seen from the free-stream turbulence spectrum near the leading edge in Figure 3. This yields about 2.9% turbulence intensity near the flat plate leading edge, matching the value in the experiments [37]. A convective boundary condition is applied at outlet and a no-slip wall boundary condition is used on the plate surface while a slip wall boundary condition is adopted on the contour surface to avoid huge separation occurring there.

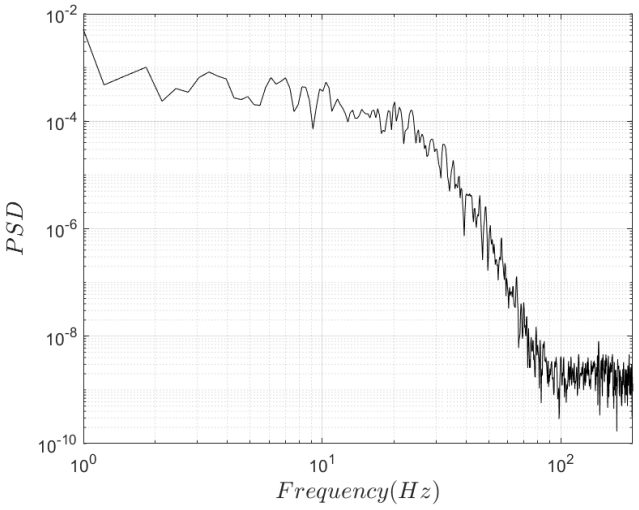

FIG. 3. Free-stream turbulence spectrum near the leading edge.

The initial calculation ran for 5 flow-through periods to give fully established flow field. Time averaged quantities were gathered over further 10 flow-through periods with samples taken at every time step. Instantaneous quantities at many locations were also collected at every time step for spectral analyses and at every 20 time steps for flow visualization. A summary of computational details of the present study can be found in Table 1 below.

Table 1. Computational details

Plate thickness	d	12.8mm
Test section length	S_o	500mm
Plate span		100mm
Inflow velocity	U_{in}	1.34m/s
Test section nominal exit velocity	U_{out}	2.5m/s
Reynolds number	Re_{S_o}	84000
Turbulence intensity	T_u	2.9
Time step size	s	1.0×10^{-4}
Mesh points		5×10^6
Nearest wall y+		< 1
CFL		<0.3

4. RESULTS AND DISCUSSION

4.1 Mean flow variables

The mean separation and reattachment locations can be identified when the mean wall shear stress reaches zero, as shown in Figure 4. The predicted mean separation and reattachment locations in the present study are at x/So ≈ 0.62 and x/So ≈ 0.87, giving a mean separation bubble length of 0.25So. The measured mean separation bubble length is about 0.31So with the mean separation and reattachment locations being x/So ≈ 0.54 and x/So ≈ 0.85 [37]. The predicted mean separation and reattachment locations in the previous LES study by Nagabhushanan *et al.* [38] are x/So ≈ 0.62 and x/So ≈ 0.86, giving a mean separation bubble length of 0.24So. The present predictions agree extremely well with the previous LES results but both LES studies under-predicted the mean separation bubble length by about 19%, which is most likely due to the difficult of reproducing exactly the same pressure gradient in the numerical simulations, causing the predicted mean separation location further downstream compared with the measured one.

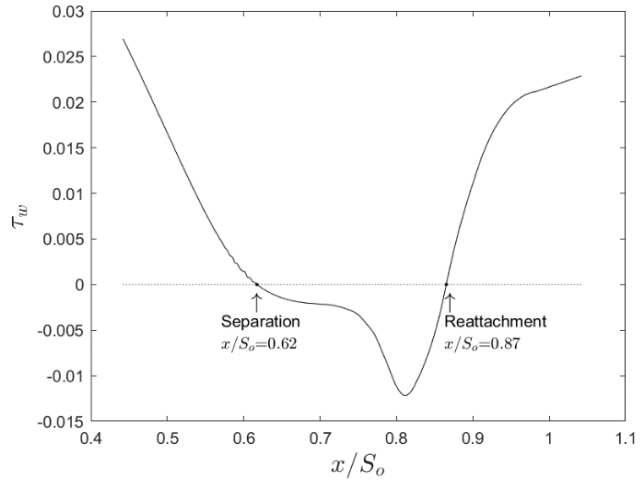

FIG. 4. Mean wall shear stress showing the separation and reattachment locations.

The normalized freestream velocity distribution (U_{fs}/U_{out}) over the upper plate surface along the streamwise direction is presented in Figure 5. The same approach used by Coull and Hodson [37] is employed here to evaluate U_{fs}. It can be seen clearly from this figure that a good agreement has been obtained between the current LES result and the experimental data. Especially in the region around x/S_o = 0.8, the current LES results show a better agreement with the experimental data than the previous LES results.

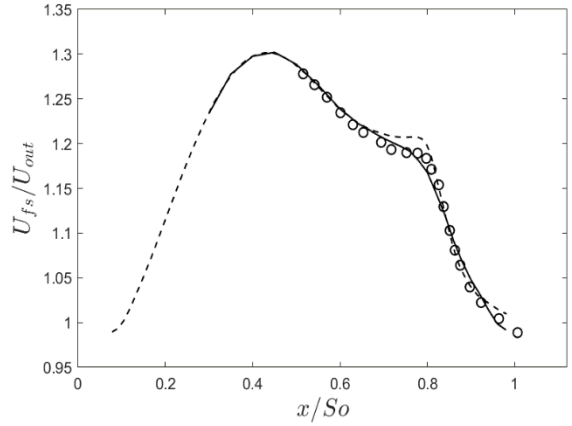

FIG. 5. Streamwise velocity distribution in the free-stream region, Solid line: current LES; symbols: Coull and Hodson [37]; dashed line: Nagabhushanon [38]

Figure 6 shows the mean streamwise velocity profiles at six streamwise locations. There is a very good agreement between the present LES results and the experimental data by Coull and Hodson [37], slightly better agreement than the previous LES result by Nagabhushanan *et al.* [38], especially around the reattachment location at x/S_o = 0.85 and 0.90. This better prediction can be attributed to the very good mesh resolution in combination with the dynamic SGS model used in the present study. It is evident from the above comparisons that the present LES has captured the flow field very well with accurate predictions of the mean flow quantities.

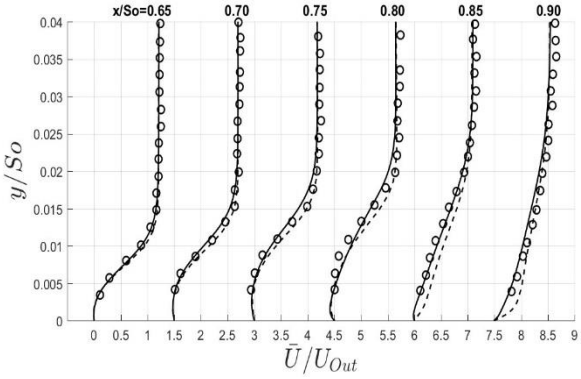

FIG. 6. Time-mean velocity profiles, x/So=0.65, 0.70, 0.75, 0.80, 0.85, 0.90. Solid line: current LES; symbols: Coull and Hodson [37]; dashed line: Nagabhushanon [38].

4.2 Instabilities and transition process

4.2.1 Instability in the boundary layer

Instantaneous data at many points were stored to obtain power spectrum density (PSD) and the highest frequency that can be resolved is 5kHz while the lowest frequency is 0.5 Hz. The estimated uncertainty of PSD is about 3%. Figure 7 shows the PSD of streamwise velocity fluctuations at ten streamwise locations and a distinct frequency peak of approximate $30U_{out}/S_o$ can be observed at several upstream locations up to the location at x/S_o=0.18. However, further downstream from x/S_o=0.22 till after the mean separation location at x/S_o=0.65 this peak disappears and no other distinct frequency is observable. This peak at upstream locations is reasonably close to the T-S wave maximum amplification frequency, $f_{TS(unstable)}\approx 25U_{out}/S_o$, evaluated at x/S_o=0.12 according to the correlation suggested by Walker [45]. This may indicate the existence of T-S wave at the upstream region of the boundary layer. However, at those streamwise locations from x/S_o=0.1 to x/S_o=0.18 the boundary

layer is under strong favourable pressure gradient and hence TS waves are very unlikely to develop at any frequencies. The pressure gradient changes from favourable to adverse at about x/S_o=0.4 and it is possible for TS waves to develop downstream of this locations but there is no distinct frequency peak appearing downstream. Furthermore the free-stream turbulence level is about 2.9% at the lead ledge, decaying to about 1.8% at x/S_o=0.4, which is still high enough to cause bypass transition (the T-S wave stage is bypassed). One distinct feature of bypass transition is the appearance of elongated streamwise streaky structures which can be clearly seen in Figure 8 presenting contours of streamwise velocity fluctuations near the wall. This is due to low-frequency contents of free-stream turbulence penetrating into the laminar boundary layer (high-frequency disturbances in the free-stream is strongly damped by the laminar shear layer, called shear sheltering) and undergo an algebraic growth (called transient growth or nonmodal growth), leading to the formation of those streaks. Throughout the analysis of the intensive data in the present study there are no other evidences showing the existence of T-S waves either.

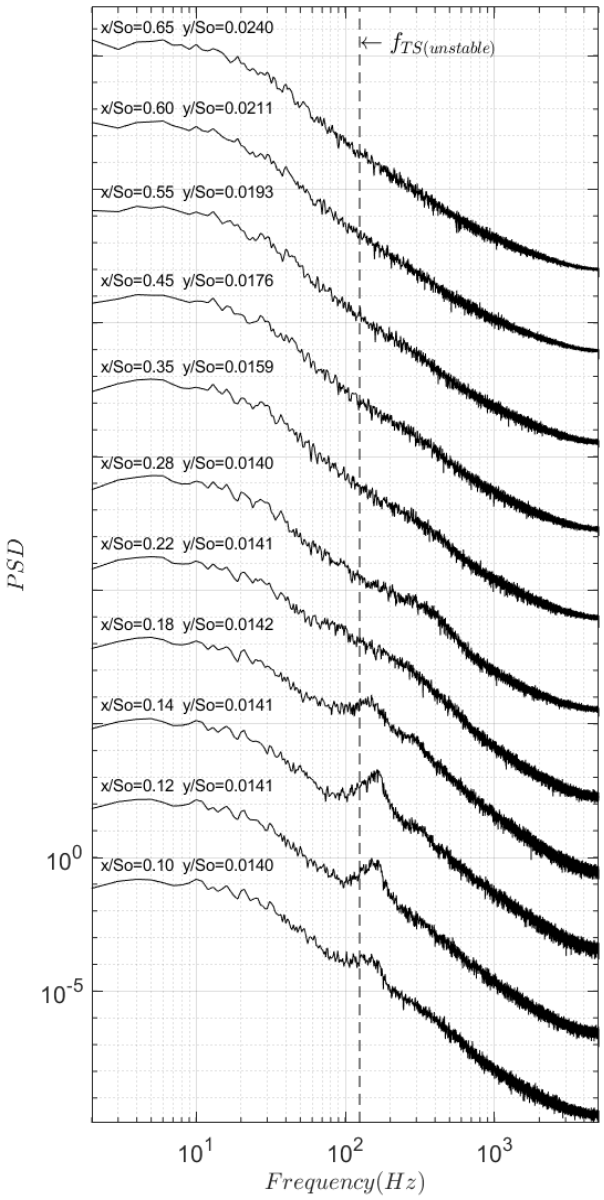

FIG. 7. PSD of streamwise velocity fluctuations at ten streamwise locations. Vertical dash line: $f_{TS(unstable)} = 25U_{out}/S_o$ predicted by T-S wave maximum amplification correlation at x/S_o=0.12.

4.2.2 Instability and transition in the separated shear layer

Despite the appearance of streaky structures which is reminiscent of bypass transition in an attached boundary layer but transition does not really occur in the attached boundary layer as no development of turbulent spots is observed before separation at x/So ≈ 0.62. This can be confirmed by the fact that the rapid growth of local maximum RMS values of resolved velocity fluctuations (v' and w') only takes place after the boundary layer separates, as shown in Figure 9. In the boundary layer before separation v' and w' do not grow at all, staying at a very low value of about 2% all the way till about $x/S_0 \approx 0.74$, well past the mean separation location at $x/S_0 \approx 0.62$ and start to grow very rapidly after $x/S_0 \approx 0.74$, reaching the overall maximum values of 21% (w') and 15% (v') at $x/S_0 \approx 0.86$. Although u' starts to grow

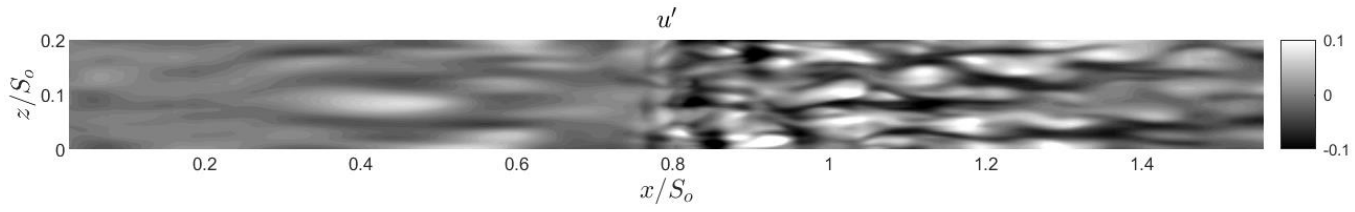

FIG. 8. Contours of streamwise velocity fluctuations near the wall

almost linearly from $x/S_0 \approx 0.2$ till about $x/S_0 \approx 0.5$ this is due to the formation and development of streaky structures (zones of forward and backward jet-like perturbations in the streamwise direction). Around the mean separation location u' grows more rapidly at a higher rate and reaches the overall maximum value of about 32% at $x/S_0 \approx 0.8$. To compare maximum RSM growth rate a simulation was performed in the present study using identical flow conditions except that the free-stream turbulence intensity was zero. It can be seen from Figure 10 that for the zero free-stream turbulence case u' starts to grow only after the separation (mean separation location is at $x/S_0 \approx 0.58$) in the absence of streaky structures, initially slowly and much more rapidly after $x/S_0 \approx 0.78$, reaching the overall maximum value of about 23% at $x/S_0 \approx 0.97$. This is quite different from the free-stream case as shown in Figure 9 where u' starts to grow in the attached boundary layer due to the streaks. However similar trends are observed for v' and w' growth in both cases, starting to grow rapidly at more or less the same locations, although the growth rate is slightly higher in the free-stream turbulence case since less distance is needed for both v' and w' to reach the overall maximum values at $x/S_0 \approx 0.86$. While for the zero free-stream turbulence case the overall maximum values for v' and w' are reached at $x/S_0 \approx 0.92$ and $x/S_0 \approx 0.97$.

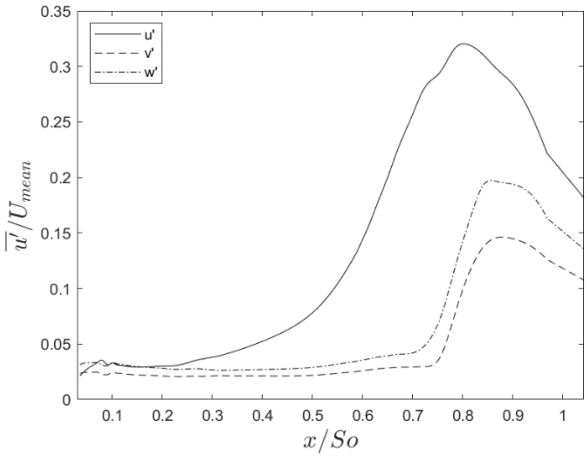

FIG. 9. Maximum RMS fluctuation along streamwise direction for the free-stream turbulence case (2.9%). Solid line: $\sqrt{u'u'}/U_{out}$, dash-line: $\sqrt{v'v'}/U_{out}$, dash-dot line: $\sqrt{w'w'}/U_{out}$

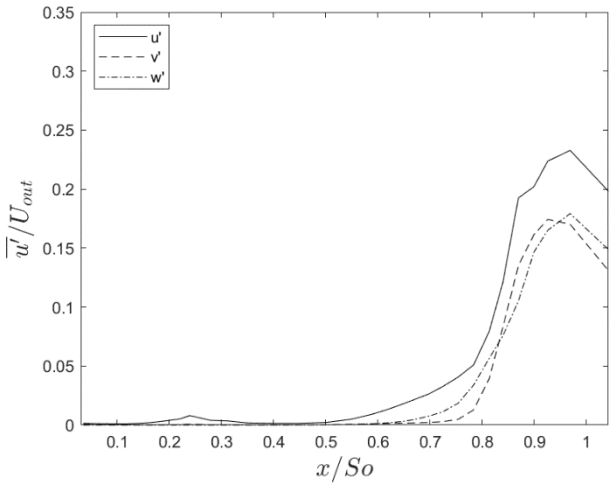

FIG. 10. Maximum RMS fluctuation along streamwise direction for the zero free-stream turbulence case. Solid line: $\sqrt{u'u'}/U_{out}$, dash-line: $\sqrt{v'v'}/U_{out}$, dash-dot line: $\sqrt{w'w'}/U_{out}$

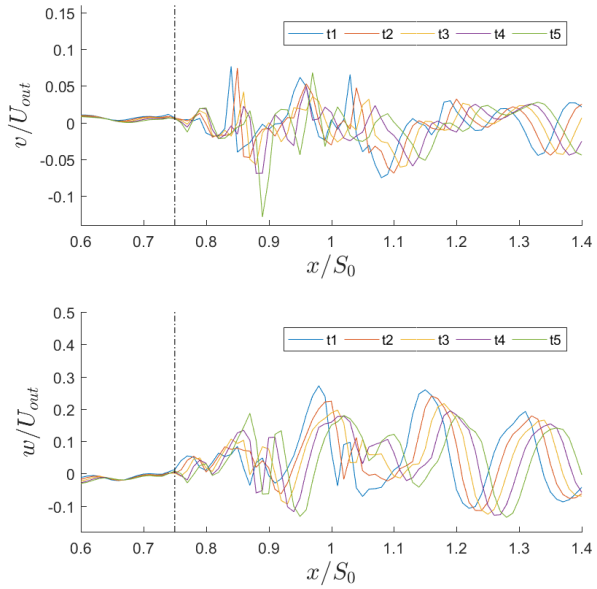

FIG. 11. Instantaneous wall normal and spanwise velocity components at five consecutive time steps along streamwise direction.

Further confirmation that transition does not occur before separation for the free-stream case is presented in Figure 11 which shows the instantaneous v and w profiles along the streamwise direction at five consecutive time steps. It can be clearly seen that the v and w profiles at five consecutive time steps are virtually the same before x/S_0=0.75, which is well into separation region, and start to diverge afterwards with fully turbulent flow

characteristics developed downstream of x/S_0=0.85. Hence in the present study transition occurs in the separated shear layer but what initiates the transition, the K-H instability or other mechanisms?

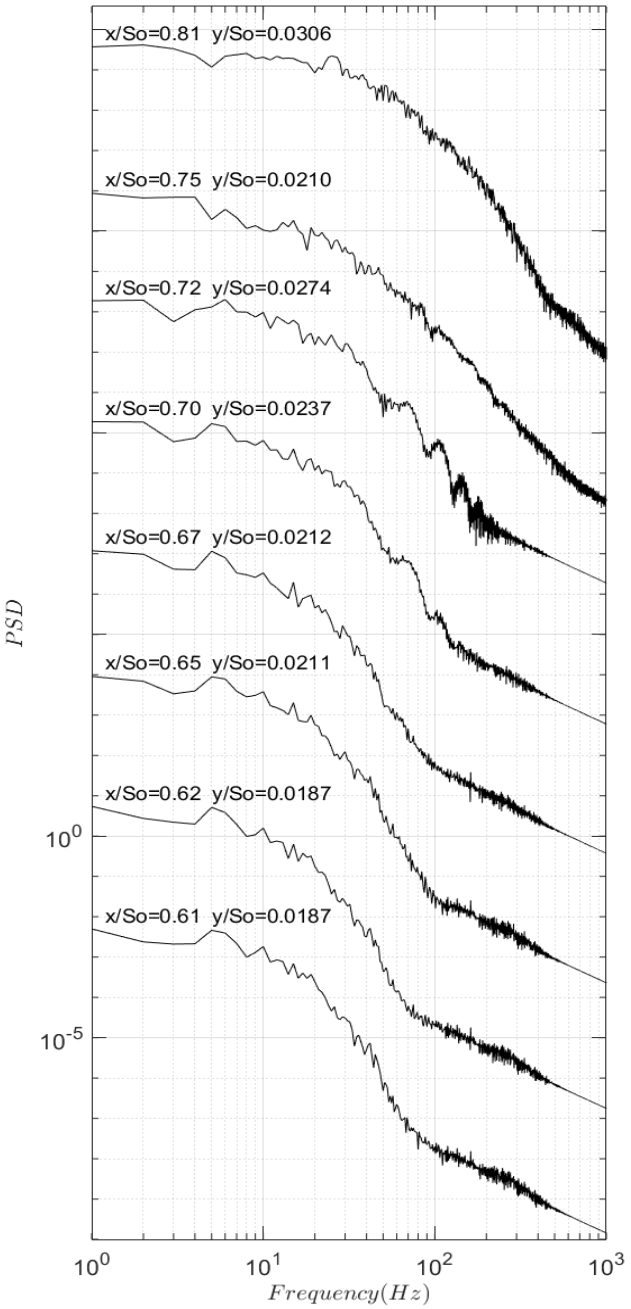

FIG. 12. PSD of streamwise velocity fluctuations at eight streamwise locations.

It was demonstrated in a DNS study of the effect of free-stream turbulence on laminar boundary layer separation and transition by Balzer and Fasel [30] that a distinct frequency peak is still clearly observable in the spectra for the highest free-stream turbulence case (2.5%) in their study, very close to the dominant frequency associated with the K-H instability in the case without free-stream turbulence. They found that the transition was due to the interaction between the K-H instability and the streaky structures formed upstream of separation. In an experimental study by Istvan and Yarusevych [31] on the effects of free-stream turbulence on transition in a laminar separation bubble it was shown that for the highest free-stream turbulence intensity case (1.99%) in their study the inviscid shear layer instability (K-H instability) is still at work. Nevertheless they identified that the streamwise streaky structures formed upstream of separation also play an important role in the transition process. In the present study under 2.9% free-stream turbulence which is higher than those in the two previous studies [30, 31], no single distinct frequency peak can be found from the PSD of streamwise velocity fluctuations at eight streamwise locations downstream from around the mean separation location as shown in Figure 12 below (spectra of v' and w' do not show any distinct peaks either).

It can also be seen from Figure 12 that there are two very small peaks around f = 70 and 103Hz at x/S_0=0.7, which becomes more apparent at x/S_0=0.72 with a third peak (f = 140 Hz) appearing at this location too but all those peaks disappear downstream at x/S0=0.75 and x/S0=0.81. The corresponding Strouhal number ($St_\theta = f \cdot \theta/\bar{U}$, where θ is the local momentum thickness) to those frequencies are 0.018, 0.032 and 0.044. The first Strouhal number (0.018) is just out of the K-H instability Strouhal number range observed in several experimental and computational studies of separated shear layers while the other two Strouhal numbers are far too large. In terms of dimensionless wave number, those frequency peaks correspond to kh = 1.36, 2.1 and 2.8, (k is the wave number and h is the local shear layer thickness). The first dimensionless wave number is slightly larger than the K-H instability dimensionless wave number range given by Simoni *et al.* [46] and by Yang and Voke [3] while the last two numbers are far too large. This is consistent with the finding using Strouhal

number, which may indicate that the K-H instability may not play a dominant role in the transition.

Those small peaks indicate that vortex shedding may still occur locally in the separated shear layer at about x/S_0=0.72. Nevertheless the vortex shedding is much weaker than the usual vortex shedding associated with the K-H instability and not at the usual frequency range either. Several studies [33 – 35] show clearly that separation is eliminated completely at higher free-stream turbulence intensity levels and transition is indeed dominated by the bypass mechanism of an attached boundary layer. However, in the present study the free-stream turbulence level is not that high and it is shown above that separation is not suppressed with transition still initiated in the separated shear layer, and further analysis of coherent structures is presented below to elucidate the transition process.

Flow visualization in previous studies [3-6, 8, 9, 12, 36, 47] reveal that in the early stage of separated boundary layer transition under low free-stream turbulence 2D spanwise vortices are formed as a result of the K-H instability, hence also called K-H rolls. To show the 2D K-H rolls a simulation was conducted in the present study using identical flow conditions except that the free-stream turbulence intensity was zero. Figure 13 presents Q iso-surfaces showing coherent structures and it can be seen clearly that 2D K-H rolls are formed initially due to the K-H instability, which get distorted downstream and breakdown to 3D structures due to a secondary instability. However, the flow structures are quite different under 2.9% free-stream turbulence intensity as shown in Figure 14 at five consecutive times. The above mentioned 2D K-H rolls are hardly observable as they are severely distorted and actually broken up in the spanwise direction due to a strong interaction of the separated shear layer with the streaky structures (grey colour) formed upstream of separation. As a result of this strong interaction between the separated shear layer and streaks, the periodic process of the usual 2D shear layer roll-up leading to vortex shedding is severely disrupted, resulting in a highly 3D shear layer roll-up, and hence a strong distinct peak associated with the K-H instability is not present. However, the broken spanwise vortices may still be shedded which can be confirmed from the shedding process as shown clearly in Figure 15. Nevertheless those severely distorted 2D spanwise vortices are shedded at different frequencies which correspond to those small peaks as shown in Figure 12. Although severely distorted and even broken those rolls may still be a kind of manifestation of the K-H instability which, however, does not play a dominant role in transition as in the low free-stream turbulence intensity case. Similar distorted 2D spanwise rolls were also observed in a previous study [48] under 2% free-stream turbulence intensity where the K-H instability was still active.

It is clear from the above analysis and discussion that the K-H instability is definitely not the only mechanism responsible for initiating transition in the present study and the streaky structures formed upstream of separation play an important role too. Transition is due to the interaction of the K-H instability and streaky structures. This is consistent with the findings by previous studies [9, 30 – 33]. Further analysis is presented below to elucidate the formation of streaky structures and how they interact with the separated shear layer.

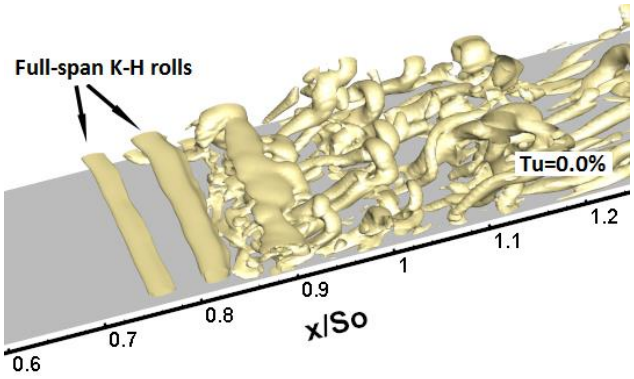

FIG. 13. Coherent flow structures without free-stream turbulence

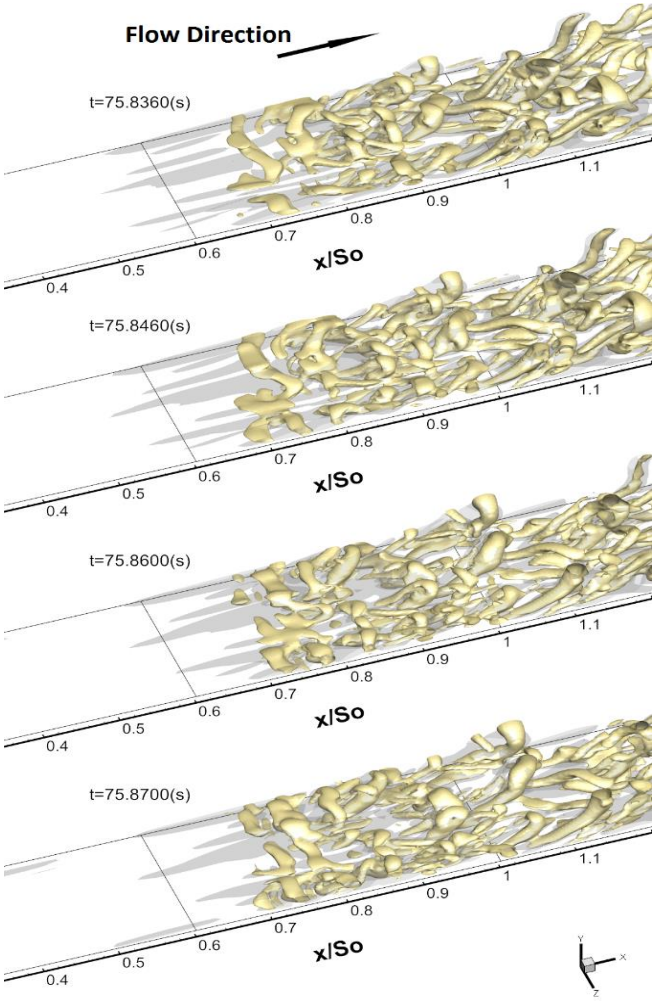

FIG. 14. Coherent flow structures at four consecutive times

Figure 16 shows the process of a streaky structure formation and its interaction with the separated shear layer. It can be seen from Figure 16A (t=75.260s) that a streaky structure is formed upstream not far away from the leading edge at $x/S_0 \approx 0.06$. The streaky structure travels downstream and gets stretched in streamwise direction with the leading edge of the streaky structure tilted upward slightly as shown in Figure 16B (t=75.308s). The streaky structure becomes more elongated in streamwise direction when travelling further downstream, and in the meantime the leading edge of the streaky structure tilts upwards further as it gets closer to the boundary layer separation location as shown in Figure 16C (t=75.328s). Finally once past the boundary layer separation location the streaky structure is lifted up and interacts with the separated shear layer as shown in Figure 16D (t=75.368s), leading to the severely distorted/broken K-H rolls as observed in Figure 14 and resulting in a much more rapid transition process compared with the transition process shown in Figure 13. One major difference in the transition process is that for the zero free-stream turbulence intensity case the initially formed 2D K-H rolls get distorted gradually with the undulation in the spanwise direction being amplified while travelling downstream. It takes quite a certain streamwise distance before the 2D rolls get severely distorted and break up into 3D structures due to a secondary instability. However, this "secondary instability stage" is absent under 2.9% free-stream turbulence intensity as the 2D K-H rolls get severely distorted and broken by the travelling streaks from upstream once they are formed, leading to the generation of significant 3D motions. Hence it is plausible to suggest that the secondary instability stage is actually "bypassed" under elevated free-stream turbulence while the K-H instability is still at work in the present study.

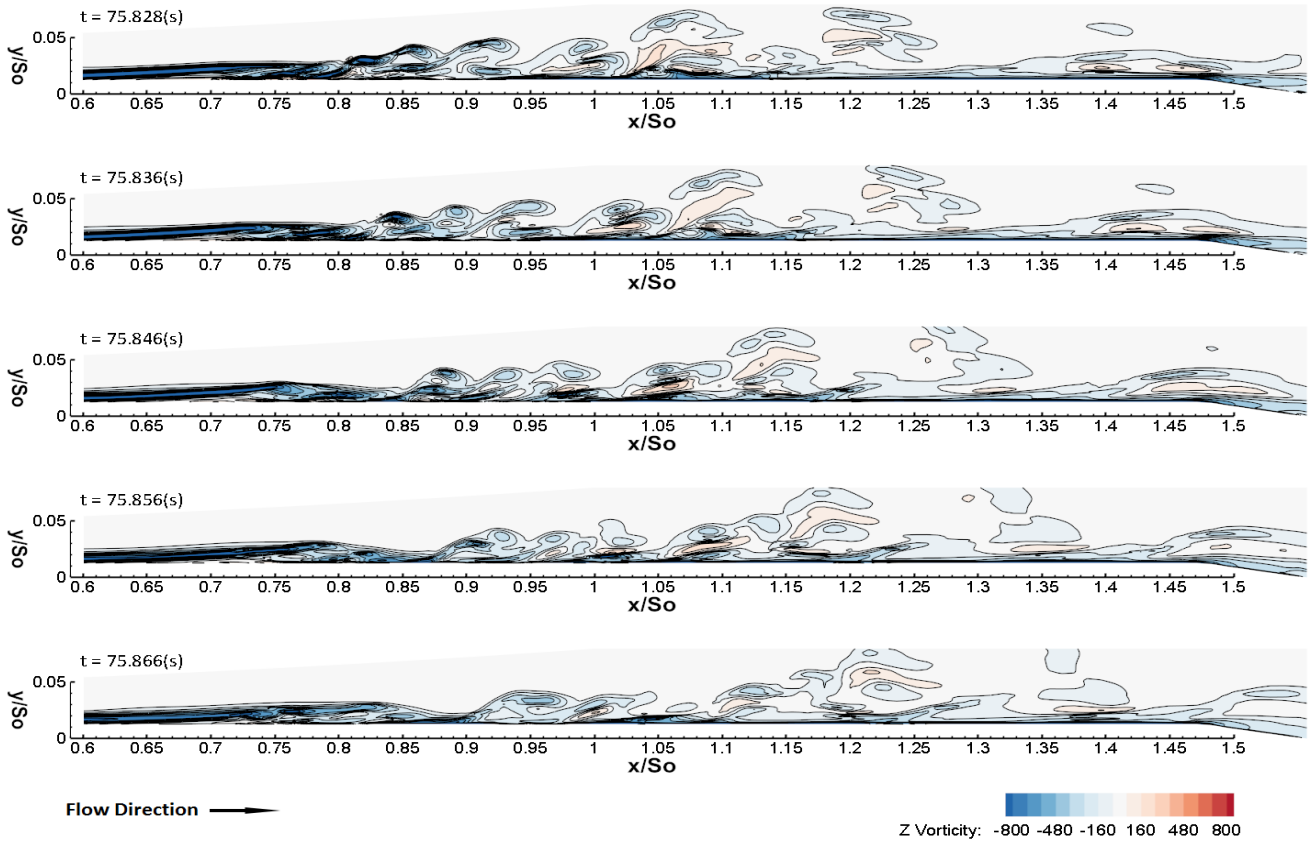

FIG. 15. Contours of instantaneous spanwise vorticity at five consecutive times showing vortex shedding process.

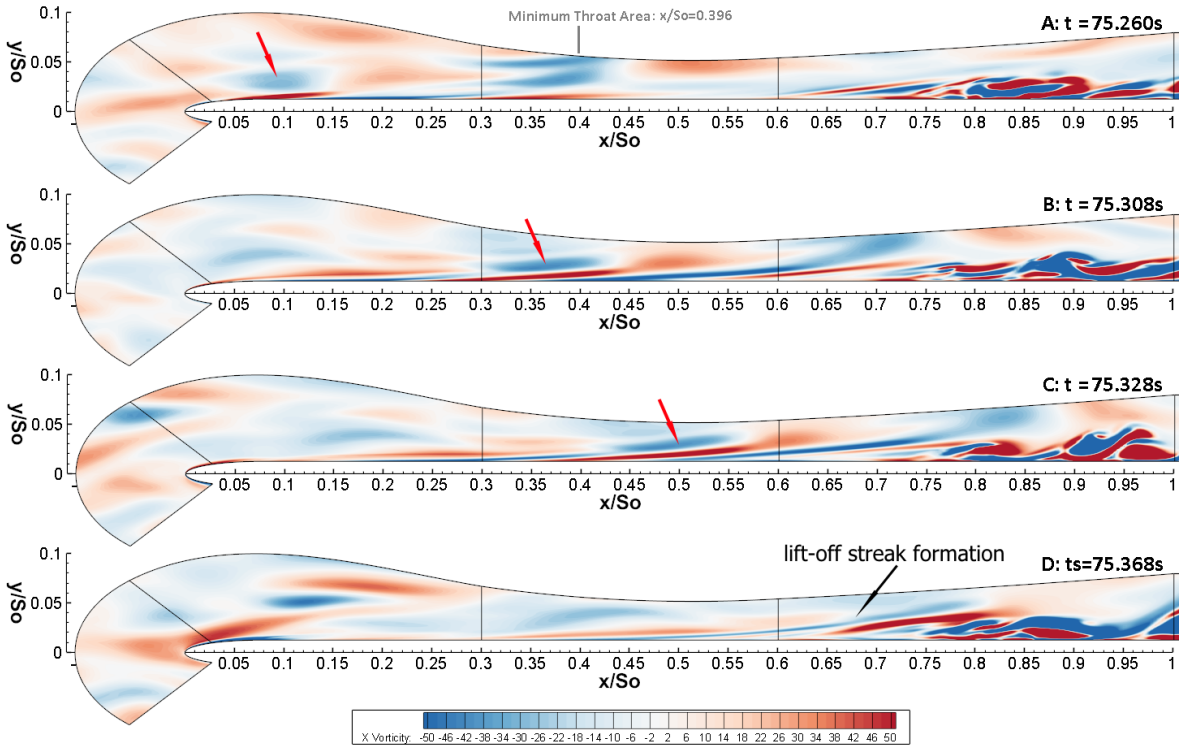

FIG. 16. Contours of instantaneous streamwise vorticity showing formation of a streaky structure and its interaction with the separated shear layer.

4.3 Discussion

It is evident in the present study that the separation bubble is not suppressed under 2.9% free-stream turbulence intensity and transition occurs in the separated shear layer. The K-H instability is still active and not bypassed. However, the K-H instability is not the only mechanism causing transition as the streamwise streaks formed upstream of separation play an important role in the transition process. The spectra show that a distinct peak associate with the K-H instability is not observable and small peaks are present at certain streamwise locations, indicating that the vortex shedding is much weaker and at different frequencies. Further analysis from flow visualization confirm that this is due to 2D K-H rolls being severely distorted and broken up, and those broken spanwise vortices are shedded at different frequencies. All those evidences suggest that the K-H instability does not play a dominant role in the transition process. Hosseinverdi and Fasel [49] reached the same conclusion in their DNS study of transition in a laminar separation bubble. They investigated the effect of free-stream turbulence intensity on the transition process and considered four case: 0.1%, 0.5%, 1% and 2%. Two mechanisms were found responsible for transition: the K-H instability and the streaky structures (K-modes). They demonstrated that for the lowest case (0.1%) the K-H instability is the dominant mechanism while in the presence of moderate free-stream turbulence intensity (0.5% – 1%) the K-H instability and K-modes contribute more or less equally to the transition process. For the highest free-stream turbulence intensity case (2%), the transition mechanism is dominated by K-modes. A similar conclusion was drawn by Istvan and Yarusevych [31] from their experimental study on transition in a laminar separation bubble formed over the suction side of an airfoil under four free-stream turbulence intensity levels (0.06%, 0.32%, 0.51%, 1.99%). They found that under low free-stream turbulence intensity spanwise rolls associate with the K-H instability are the main contributors to the overall energy of velocity fluctuations. However, the contribution from the spanwise rolls reduces when the level of free-stream turbulence intensity increases. For the highest free-stream turbulence intensity case (1.99%) the streaks contribute more to the overall energy of velocity fluctuations than spanwise rolls. The diminishing role played by the coherent K-H rolls with increasing free-stream turbulence intensity was also confirmed by Simoni *et al*. [32] in an experimental study on the structure and dynamic properties of a laminar separation bubble under three free-stream turbulence intensity levels (0.65%, 1.2% and 2.87%). Their Proper Orthogonal Decomposition (POD) analysis show that when the free-stream turbulence intensity level increases, less energy is captured by the first POD modes since the transition process is characterized by the presence of a "broader band" of structures.

One new finding is that the secondary instability stage in the transition process of a separation bubble under low free-stream turbulence is actually "bypassed" in the present study under elevated free-stream turbulence intensity of 2.9%. Transition occurs much more rapidly and over a shorter streamwise distance. It is also worth noting that the term "bypassed transition" in laminar separation bubbles could be misleading as the K-H instability is still at work as long as separation occurs. However, at sufficiently high free-stream turbulence intensity level the K-H instability is not relevant anymore because separation is suppressed and the usual bypass transition occurs in an attached boundary layer. In such a case it is not really meaningful anymore to say that the K-H instability is bypassed as the separated shear layer does not exist at all.

5. CONCLUSION

The transition process in a separation bubble induced by an adverse pressure gradient on a flat plate with an elliptical leading edge under 2.9% free-stream turbulence intensity has been investigated numerically. LES approach with a dynamic sub-grid-scale model has been employed and mesh has been properly refined with a very good resolution in important flow regions to minimize the effect of sub-grid-scale modelling. The predicted mean results agree well with the experimental data and a previous LES predictions.

Streamwise streaky structures are formed shortly downstream of the leading edge due to the elevated free-stream turbulence and significant streamwise velocity fluctuations (u') are observed in the

attached boundary layer as a result of the streaks. Those streaks may signify an onset of bypass transition in the attached boundary layer before separation. However, no turbulent spots are found before separation and the other two velocity fluctuations (v', w') are very low and only start to increase after separation. It is evident that transition occurs in the separated shear layer and is caused by two mechanisms: the streamwise streaks (K-modes) and the K-H instability. Flow visualization clearly show that 2D coherent spanwise vortical structures associated with the K-H instability are severely distorted and broken up in spanwise direction, resulting in highly 3D shear layer roll-up which leads to weaker vortex shedding at different frequencies with several observable small peaks in spectra. This is in sharp contrast with the low free-stream turbulence case where a distinct peak associated with the K-H instability would appear in spectra. The analysis in the present study suggests that the K-H instability is not the dominant mechanism causing transition under 2.9% free-stream turbulence intensity. This is consistent with several previous studies as discussed above.

The transition process is more rapid and over a shorter streamwise distance due to the dominant role played by the streaks, which severely disrupt and break the K-H rolls once they are formed, leading to significant 3D motions very rapidly. The usual secondary instability stage under low free-stream turbulence intensity where very coherent 2D spanwise rolls get distorted gradually and eventually broken into 3D structures has been bypassed.

REFERENCES

[1] P.R. Spalart, M.K.H. Strelets, Mechanisms of transition and heat transfer in a separation bubble, J. Fluid Mech. 403 (2000) 329-349.

[2] Z. Yang, P.R. Voke, On early stage instability of separated boundary layer transition. In: Dopazo, C. (Ed), Advances in Turbulence VIII. CIMNE, Spain, 2000, pp. 145-148.

[3] Z. Yang, P.R. Voke, Large-eddy simulation of boundary layer separation and transition at a change of surface curvature, J. Fluid Mech. 439 (2001) 305-333.

[4] Z. Yang, Large-scale structures at various stages of separated boundary layer transition, International Journal for Numerical Methods in Fluids 40 (2002) 723-733.

[5] I.E. Abdalla, Z. Yang, Numerical study of the instability mechanism in transitional separating-reattaching flow, Int. J. Heat and Fluid Flow 25 (2004) 593-605.

[6] I.E. Abdalla, M.J. Cook, Z. Yang, Numerical study of transitional separated-reattached flow over surface-mounted obstacles using Large-Eddy Simulation, International Journal for Numerical Methods in Fluids 54 (2007) 175-206.

[7] S. Burgmann, J. Dannemann, W. Schroder, Time-resolved and volumetric PIV measurements of a transitional separation bubble on an SD7003 airfoil, Experiments in Fluids 44 (2008) 609-622.

[8] I.E. Abdalla, Z. Yang, M.J. Cook, Computational analysis and flow structure of a transitional separated–reattached flow over a surface mounted obstacle and a forward-facing Step, International Journal of Computational Fluid Dynamics 23 (2009) 25-57.

[9] B.R. McAuliffe, M.I. Yaras, Transition mechanisms in separation bubbles under low- and elevated-freestream turbulence, Journal of Turbomachinery 132 (2010) 011004.

[10] F. Satta, D. Simoni, M. Ubaldi, P. Zunino, and F. Bertini, Experimental investigation of separation and transition processes on a high- lift low-pressure turbine profile under steady and unsteady inflow at low Reynolds number, Journal of Thermal Science 19 (2010) 26-33.

[11] J. Dahnert, C. Lyko, and D. Peitsch, Transition mechanisms in laminar separated flow under simulated low pressure turbine aerofoil conditions, Journal of Turbomachinery 135 (2012) 011007.

[12] Z. Yang, Numerical study of instabilities in separated-reattached flows, Int. J. Comp. Meth. and Exp. Meas. 1 (2013) 116–131.

[13] J. Serna, B.J. Lazaro, on the laminar region and the initial stages of transition in transitional separation bubbles, European Journal of Mechanics B/Fluids 49 (2015) 171-183.

[14] M. Lang, U. Rist, S. Wagner, Investigations on controlled transition development in a laminar separation bubble by means of LDA and PIV, Experiments in Fluids 36 (2004) 43-52.

[15] R.J. Volino, D.G. Bohl, Separated flow transition mechanism and prediction with high and low free stream turbulence under low pressure turbine conditions, in: Proceedings of ASME Turbo Expo 2004: Power for Land, Sea, and Air, Vienna, Austria, June 14–17, 2004, Paper No. GT2004-53360.

[16] S.K. Roberts, M.I. Yaras, Boundary-layer transition affected by surface roughness and free-stream turbulence, Journal of Fluids Engineering 127 (2005) 449-457.

[17] S.K. Roberts, M.I. Yaras, Large-eddy simulation of transition in a separation bubble, Journal of Fluids Engineering 128 (2006) 232–238.

[18] O. Marxen, M. Lang, U. Rist, Discrete linear local eigenmodes in a separating laminar boundary layer, J. Fluid Mech. 711 (2012) 1-26.

[19] P.R. Voke, Z. Yang, Numerical study of bypass transition, Physics of Fluids 7 (1995) 2256-2264.

[20] P. Andersson, L. Brandt, A. Bottaro, D.S. Henningson, On the breakdown of boundary layer streaks, J. Fluid Mech. 428 (2001) 29-60.

[21] R.G. Jacobs, P.A. Durbin, Simulations of bypass transition, J. Fluid Mech. 428 (2001) 185-212.

[22] T.A. Zaki, P.A. Durbin, Mode interaction and the bypass route to transition, J. Fluid Mech. 531 (2005) 85-11.

[23] P. Schlatter, L. Brandt, H.C. de Lange, D.S. Henningson, On streak breakdown in bypass transition, Physics of Fluids 20 (2008) 101505.

[24] Z. Xu, Q. Zhao, Q. Lin, J. Xu, Large eddy simulation on the effect of free-stream turbulence on bypass transition, Int. J. Heat Fluid Flow 54 (2015) 131-142.

[25] X. Wu, P. Moin, J-P. Hickey, Boundary layer bypass transition, Physics of Fluids 30 (2014) 091104.

[26] A. Zhang, M. Dong, Y. Zhong, Receptivity of secondary instability modes in streaky boundary layers, Physics of Fluids 30 (2018) 114102.

[27] G.J. Walker, The role of laminar-turbulent transition in gas turbine engines: A discussion, Journal of Turbomachinery 115 (1993) 207-216.

[28] Z. Yang, Bypass transition in separated-reattached flows under elevated free-stream turbulence, The 6th International Symposium on Jet Propulsion and Power Engineering, Beijing, China, October 16-18, 2017, Paper No. 2017-ISJPPE-0010.

[29] Z. Yang, On bypass transition in separation bubbles: a review, Propulsion and Power Research 8 (2019) 23-34.

[30] W. Balzer, H.F. Fasel, Numerical investigation of the role of free-stream turbulence in boundary-layer separation, J. Fluid Mech. 801 (2016) 289–321.

[31] M.S. Istvan, S. Yarusevych, Effects of free-stream turbulence intensity on transition in a laminar separation bubble formed over an airfoil, Exp. Fluids 59 (2018) 52: 1-21.

[32] D. Simoni, D. Lengani, M. Ubaldi, P. Zunino, M. Dellacasagrande, Inspection of the dynamic properties of laminar separation bubbles: free-stream turbulence intensity effects for different Reynolds numbers, Exp Fluids 58(2017) 66:1-14.

[33] T.A. Zaki, J.G. Wissink, W. Rodi, P.A. Durbin, Direct numerical simulations of transition in a compressor cascade: the influence of free-stream turbulence, J. Fluid Mech. 665 (2010) 57-98.

[34] Y. Dong, N.A. Cumpsty, Compressor blade boundary layer: part 2 measurements with incident wakes, Journal of Turbomachinery 112 (1990) 231–241.

[35] J.G. Wissink, DNS of separating, low Reynolds number flow in a turbine cascade with incoming wakes. Int. J. Heat and Fluid Flow 24 (2003) 626–635.

[36] M. langari, Z. Yang, Numerical study of the primary instability in a separated boundary layer transition under elevated free-stream turbulence, Physics of Fluids 25 (2013) 074106.

[37] J. Coull, H. Hodson, Unsteady boundary layer transition in low-pressure turbines, J. Fluid Mech. 681 (2011) 370–410.

[38] V. Nagabhushanan, P. Tucker, R. Jefferson, J. Coull, Large eddy simulation in low-pressure turbines: Effect of wake at elevated free-stream turbulence, Int. J. Heat and Fluid Flow 43 (2013) 85–89.

[39] M. Germano, M. Piomelli, P. Moin, and W.H. Cabot, A dynamic subgrid-scale eddy viscosity model, Phys. Fluids A 3 (1991) 1760-1765.

[40] D. K. Lilly, A proposed modification of the Germano subgrid-scale closure method, Phys. Fluid A 4 (1992) 633-635.

[41] M. langari, Z. Yang, G. Page, Large-eddy simulation of transitional flows using a collocated grid, International Journal of Computational Fluid Dynamics 27 (2013) 189-200.

[42] C. Pokora, W. McMullan, G. Page, and J. McGuirk, Influence of a numerical boundary layer trips on spatial-temporal correlations within LES of a subsonic jet, The 17th AIAA/CEAS Aeroacoustics Conference, Portland, Oregon, 2011, AIAA Paper No. 2011-2920.

[43] G. R. Tabor, M. H. Baba-Ahmadi, Inlet conditions for large eddy simulation: A review, Computers & Fluids 39 (2010) 553-567.

[44] Z. Yang, Large-eddy simulation: Past, present and the future, Chinese Journal of Aeronautics 28 (2015) 11 - 24.

[45] G. Walker, Transitional flow on axial turbomachine Blading, AIAA J. 27 (1989) 595-602.

[46] D. Simoni, M. Ubaldi, P. Zunino, Experimental investigation of flow instabilities in a laminar separation bubble, Journal of Thermal Science 23 (2014) 203-214.

[47] Z. Yang, Numerical study of transition process in a separated boundary layer on a flat plate with two different leading edges, WSEAS Transactions on Applied and Theoretical Mechanics 7 (2012) 49-58.

[48] Z. Yang, I. E. Abdalla, Effects of free-stream turbulence on large-scale coherent structure of a separated boundary layer transition, International Journal for Numerical Methods in Fluids 49 (2005) 331-348.

[49] S. Hosseinverdi, H. F. Fasel, Laminar-turbulent transition in a laminar separation bubble in the presence of free-stream turbulence, Procedia IUTAM 14 (2015) 570-579.